INSTITUTE OF PHYSICS PUBLISHING NANOTECHNOLOGY
Nanotechnology **16** (2005) 267–272 doi:10.1088/0957-4484/16/2/015

Morphologies and microstructures of nano-sized Cu_2O particles using a cetyltrimethylammonium template

Huairuo Zhang, Chengmin Shen, Shutang Chen, Zhichuan Xu, Fusheng Liu, Jianqi Li and Hongjun Gao[1]

Beijing National Laboratory for Condensed Matter Physics, Institute of Physics, Chinese Academy of Sciences, Beijing 100080, People's Republic of China

E-mail: hjgao@aphy.iphy.ac.cn

Received 5 November 2004, in final form 20 December 2004
Published 13 January 2005
Online at stacks.iop.org/Nano/16/267

Abstract
Hollow polyhedra and cubes of nanostructured Cu_2O particles have been synthesized by reduction of $CuSO_4$ with ascorbate acid in the solution phase. The nanostructures were obtained when the cetyltrimethylammonium (CTAB) concentration ranged from 0 to 0.03 M in the presence of NaOH. Structural characterizations, by means of x-ray photoelectron spectroscopy (XPS) for measuring Cu valence states and by electron microscopy for microstructure and chemical analyses, suggest that most Cu_2O nanoparticles are covered with a thin CuO shell arising possibly from reaction of the adsorbed oxygen on the Cu_2O particle surface. The blue shift is observed as microstructures of Cu_2O nanoparticles changed from cubic to hollow in ultraviolet and visible (UV–visible) absorption spectra. Both the Cu_2O hollow and cubic nanostructures show certain quantum-confined effects. A cationic CTAB template mechanism is proposed to interpret the formation of the Cu_2O nanoparticles.

1. Introduction

Shape and size are important factors in determining the structural, physical and chemical properties of nanoparticles [1–3]. Shape-controlled synthesis of nanoparticles has become a focus point, as different morphologic nanoparticles could have different electronic, optic and magnetic properties from that observed in their spherical counterpart. Semiconductor nanoparticles have been made in various shapes such as triangles, rods, cubes and tetrapods for potential application and for quantum confinement studies [4, 5]. Cu_2O is a p-type semiconductor with a direct bandgap of ∼2.17 eV, which makes it a promising material in the application of solar energy and catalysis [6, 7]. In recent years Cu_2O nanomaterials with different structures have been synthesized by various methods [8–12]. The notable hollow nanostructure is of current interest due to its possible application in many areas of modern science and technology, such as catalysis, drug delivery systems, chromatography, energy storage and microelectronics [13, 14]. In the present work, various nanostructured Cu_2O particles were synthesized by using CTAB as a template through a simple one-step route. The influence of CTAB concentration on the structure of Cu_2O nanoparticles was investigated.

2. Experimental details

2.1. Materials

Cetyltrimethylammonium (CTAB, ACROS), copper sulfate ($CuSO_4$, Beijing Chemicals), sodium hydroxide (NaOH, Beijing Chemicals) and ascorbate acid (ACROS) were used. All aqueous solutions were prepared with high-purity deionized water.

2.2. Synthesis of Cu_2O nanoparticles

Nanostructured Cu_2O nanoparticles with different structures were synthesized using an extended solution phase method originally reported to synthesize nanocubes [8]. In a typical experiment, a set of solutions were prepared by adding 0.25 ml

[1] Author to whom any correspondence should be addressed.

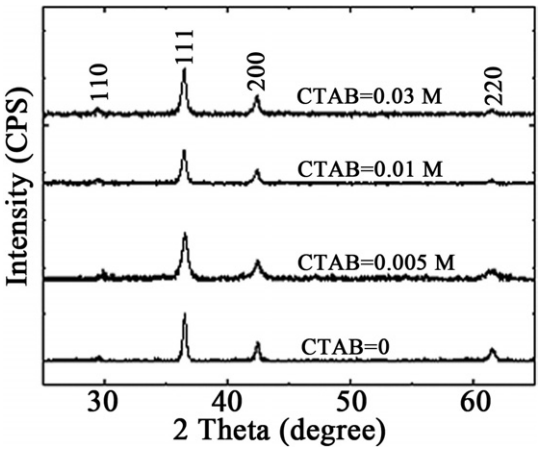

Figure 1. X-ray powder diffraction data of the as-prepared nanoparticles.

of 0.01 M aqueous $CuSO_4$ to 9.0 ml of aqueous CTAB solutions with a concentration of 0–0.03 M. Next, 0.50 ml of a 0.10 M ascorbate acid solution was added into the Cu^{2+}–CTAB mixture solutions. The solutions were heated in a water bath from room temperature to 55 °C, and kept for 5 min at this temperature. Then, 0.2 ml of a 0.5 M aqueous NaOH solution was added into the mixture solutions. The solutions were kept at 55 °C for 5 min, then were removed from heat and allowed to cool to room temperature for about 30 min. The particles were separated from the solutions by centrifugation and washed with deionized water to remove the surfactant.

2.3. Characterization

X-ray diffraction (XRD) data used for structure analysis was collected using a Rigaku D/max 2500 diffractometer with Cu Kα radiation. A step scan mode was employed with a step width of 0.02° and a sampling time of 1 s. A VG-ESCALAB-5 x-ray photoelectron spectrometer with Mg Kα exciting radiation was used to perform the surface constituent analyses. An FEI XL30 SEM and an FEI Tecnai F20 TEM were used to perform the microstructure analysis. A Cary 1E UV–vis spectrometer was used to perform absorption spectroscopy analysis.

3. Results and discussion

Figure 1 shows a set of typical XRD data collected from the as-prepared samples with CTAB concentration in the range 0–0.03 M. All clear diffraction peaks can be assigned to the cubic Cu_2O structure with the lattice parameter of 4.269 Å (standard PDF data: No. 05-0667). The average size of the grains comprising the nanoparticles in each sample have been roughly estimated from the (111) reflection peaks by using the Scherrer formula; we get 11.8, 7.5, 8.2 and 9.4 nm corresponding to CTAB concentrations of 0, 0.005, 0.01 and 0.03 M, respectively. The results indicate that the grains become gradually larger with increasing CTAB concentration from 0.005 to 0.03 M. However, the average grain size of nanoparticles prepared without CTAB is apparently larger than that of nanoparticles prepared with CTAB. Figure 2(a) shows an XPS spectrum of Cu $2P_{3/2}$ core level acquired

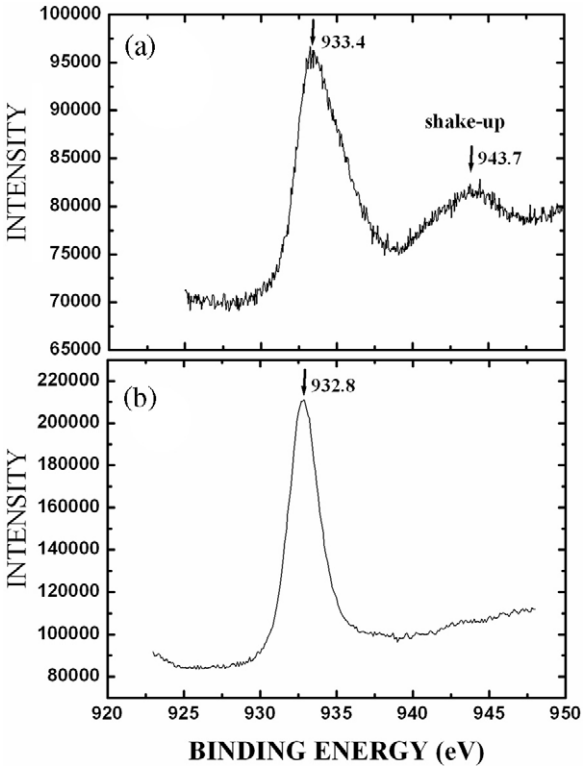

Figure 2. Cu $2P_{3/2}$ XPS data of nanoparticles taken (a) from the initial surface, identified as the cupric CuO phase, and (b) from the sample after 2 min 2 keV Ar^+ sputtering, identified as the pure cuprous Cu_2O phase.

from a deposited nano-Cu_2O sample prepared with CTAB concentration of 0.03 M. The $2P_{3/2}$ peak at 933.4 eV and the shake-up at 943.7 eV (∼10 eV away) are in good agreement with the spectral feature of Cu^{2+} [15, 16]. Then, we milled the sample by 2 keV Ar^+ sputtering for 2 min, and got the other spectrum as shown in figure 2(b). As we can see, the $2P_{3/2}$ peak shifts down to 932.8 eV with the disappearance of shake-up, which perfectly fits with the feature of the Cu^+ spectrum. These facts suggest that a thin layer of CuO possibly covers the Cu_2O nanoparticles in the as-grown samples. Further evidence supporting these microstructure properties was obtained from element mapping observations which indicate that the surface layer of nanoparticles is rich in oxygen even in high vacuum. It is also noted that this structural phenomenon shows certain similarities with the activated reactive evaporation (ARE) nanophase which suggested that the stabilization of the cubic Cu_2O nanophase is enhanced by the formation of a monoclinic CuO surface layer [17]. The element mapping analyses of O and Cu were performed on nanocubes prepared with CTAB concentration of 0.03 M. The mapping images of Cu_2O nanoparticles are shown in figures 3(a)–(c). The O element mapping image (figure 3(b)) of Cu_2O particles shows notable contrast changes depending on the particle size. This phenomenon is considered to result from the alternation of the fraction of the surface layers with high O concentration, this fraction apparently increases with the decrease of the particle size. As a result, uniform contrast in figure 3(b) is observed on certain small particles. These results demonstrate that the oxygen concentration is evidently rich on

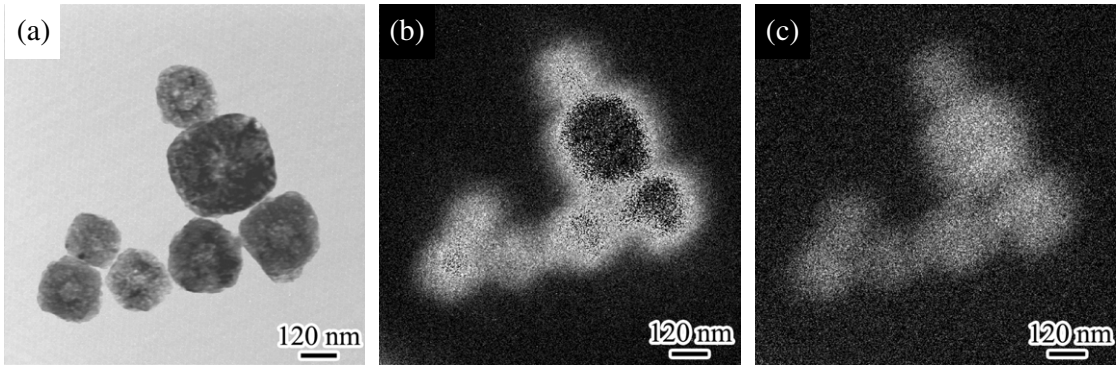

Figure 3. (a) Bright-field TEM image of nanocubes prepared with 0.03 M CTAB. Energy filtered images showing the distributions of (b) the O element and (c) the Cu element in the nanocubes.

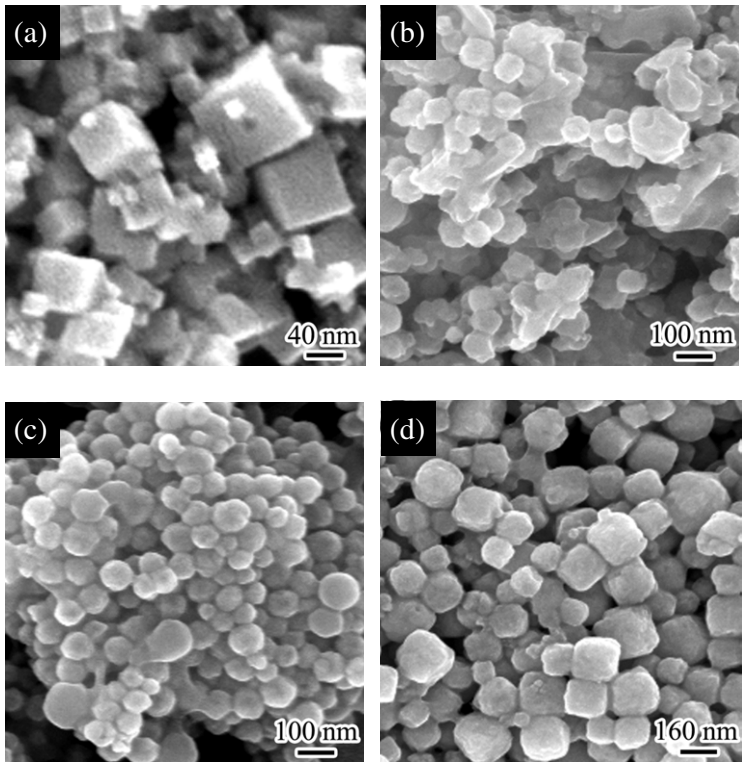

Figure 4. SEM images of nanoparticles: (a) prepared without CTAB. (b)–(d) prepared with CTAB concentration of 0.005, 0.01 and 0.03 M, respectively.

the nanocubes' surfaces, which is believed to be connected to the surface oxidizing from Cu_2O into CuO, as discussed above. In addition, we have performed electron diffraction analysis simultaneously on many particles, and we cannot find the diffraction rings from the CuO structure; this fact suggests that the CuO layer is probably amorphous.

Figure 4 is a set of typical SEM images of the Cu_2O nanoparticles prepared at different CTAB concentrations. The nanoparticles in figure 4(a) prepared without CTAB are nanocubes of poor size distribution with the edge length ranging from 20 to 100 nm. However, the nanoparticles prepared at CTAB concentrations of 0.005, 0.01 and 0.03 M in general are uniform in size and show up as irregular polyhedra or nanocubes, as illustrated in figures 4(b)–(d), and the size of the nanoparticles increases with the increase in CTAB concentration. In lower concentrations of CTAB (from 0.005 to 0.01 M), the morphology of Cu_2O nanoparticles is mainly irregular polyhedra. On the other hand, it is noted that the grain shapes of Cu_2O nanoparticles change to cubic as the concentration of CTAB increases up to 0.03 M.

In order to better understand the microstructure of these nanoparticles, we have performed systematic TEM investigations on different samples. Figures 5(a)–(d) show a series of TEM images taken from Cu_2O nanoparticles prepared at different CTAB concentrations. A large fraction of the nanocubes prepared without CTAB have complex porous structure (see figure 5(a)). Nanoparticles prepared with low CTAB concentrations of 0.005 and 0.01 M (figures 5(b) and (c)) show clear contrast changing from the particle edge to the centre area, which is believed to arise from the evident hollow nature [18]. These Cu_2O hollow nanoparticles are uniform and have dimensions of 40–60 nm. The wall thickness is estimated

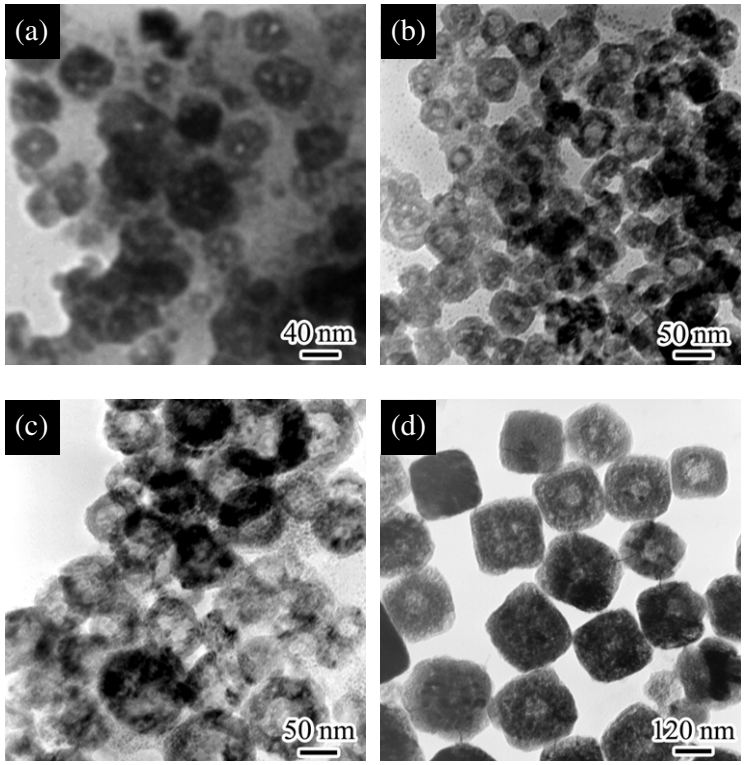

Figure 5. (a) Porous nanocubes prepared without CTAB. ((b), (c)) Hollow nanoparticles prepared with 0.005 and 0.01 M CTAB, respectively. (d) Porous nanocubes prepared with 0.03 M CTAB.

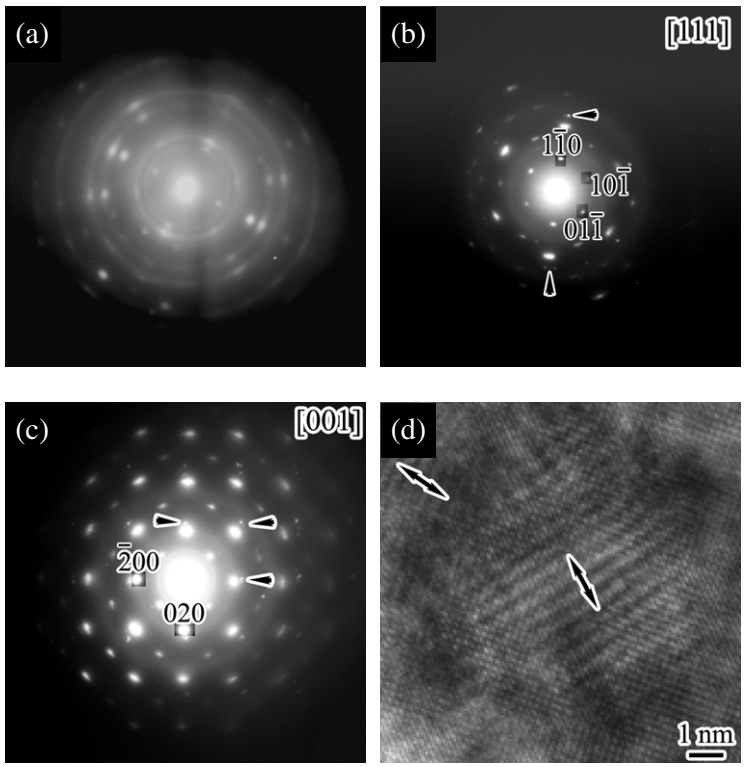

Figure 6. ((a)–(c)) Typical SAEDs of individual nanoparticles corresponding to figures 5(a)–(d), respectively. (d) A typical HRTEM image of a nanoparticle, the moiré fringes indicating the adsorbed small particles on the surface.

to be around 10 nm. Moreover, our experimental results suggest that the sizes and morphologies of the nanoparticles can be controlled by CTAB concentration. Figure 5(d) shows the TEM image of the nanoparticles prepared under CTAB concentration of 0.03 M. The particles in the present case have the shape of nanocubes.

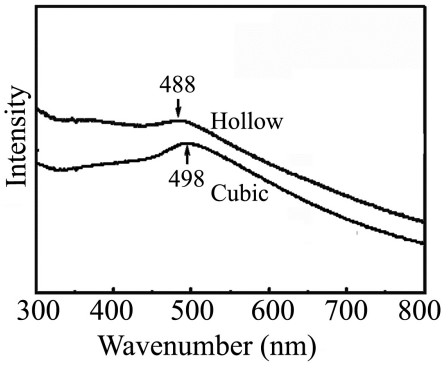

Figure 7. UV–visible absorption spectra of different morphologic Cu_2O nanoparticles.

Selected area electron diffraction (SAED) observations have been performed for checking the crystal structures of the Cu_2O nanoparticles in each sample. Figure 6(a) shows a typical SAED pattern taken from a porous particle as shown in figure 5(a); it is found that these nanoparticles in general are composed of grains aggregated randomly. With the introduction of CTAB, the crystallization of nanoparticles becomes gradually better. Figure 6(b) is a typical SAED pattern of a hollow nanoparticle prepared at low CTAB concentration which indicates a highly preferred ⟨111⟩ orientation texture structure; nanocubes prepared at high CTAB concentration (0.03 M) are found to be well crystallized along the ⟨001⟩ orientation. The broadened and streaked diffraction spots demonstrate the presence of a high density of structural defects in the crystal. It is also noted that additional weak diffraction spots (see the arrowheads in figures 6(b) and (c)) commonly appear in the electron diffraction patterns, these weak spots actually arise from small particles adsorbed on the nanoparticle's surface, as also revealed in the HRTEM image of figure 6(d). This image clearly exhibits the presence of moiré fringes due to the superimposed nanocrystals which were not incorporated into the nanoparticle completely.

The UV–visible absorption spectra for understanding the properties of atomic coupling within the nanoparticles have also been measured briefly as shown in figure 7. These UV spectra were taken from different morphologic Cu_2O particles dispersed in aqueous solution. A broad absorption peak at about 488 nm (2.54 eV) corresponds to Cu_2O hollow nanoparticles prepared at CTAB concentration of 0.005 M. When the CTAB concentration increased to 0.03 M, the absorption peak shifted to 498 nm (2.49 eV), implying that cubic nanoparticles have relatively stronger Cu_2O–Cu_2O interaction due to the improvement of crystallization of Cu_2O in the cubic nanoparticles. Comparison with bulk Cu_2O ($E_{\text{g bulk}} = 2.17$ eV), Cu_2O hollow nanoparticles ($E_{\text{g hollow}} = 2.54$ eV) and cubic nanoparticles ($E_{\text{g cube}} = 2.49$ eV) both show much larger blue shift effects in connection with the quantum-confined effects arising from the low dimensional nanocrystals comprising the hollow or cubic Cu_2O particles [19].

Figure 8 shows a schematic illustration of a possible mechanism for the formation of hollow nanoparticles. The surfactant (CTAB) molecules, within the aqueous solution of low CTAB concentration, primarily form a monolayer structure, then the monolayer structure changes progressively into micelles as the solution is gradually heated (step (a)). The Cu^{2+} ions (from solution) form Cu–Br ligands (Br^- from CTAB) by electrostatic interactions and are dispersed in the outward end of the micelles. This leads to the migration of Cu^{2+} ions from the surrounding solution and enrichment of the surface of the micelles (step (b)). The ascorbic acid reduces Cu^{2+} ions to form Cu_2O nuclei on the surface of the micelles as NaOH solution is added into hot solution (step (c)). Then, the growth of the nuclei was continued by addition of Cu_2O containing species to the surface of the Cu_2O particles, which formed a compact Cu_2O layer on the surface of the micelles (step (d)). On the other hand, the nucleated particles always evolve into polyhedral particles mirroring the crystal structure, so hollow polyhedral nanoparticles assembled by

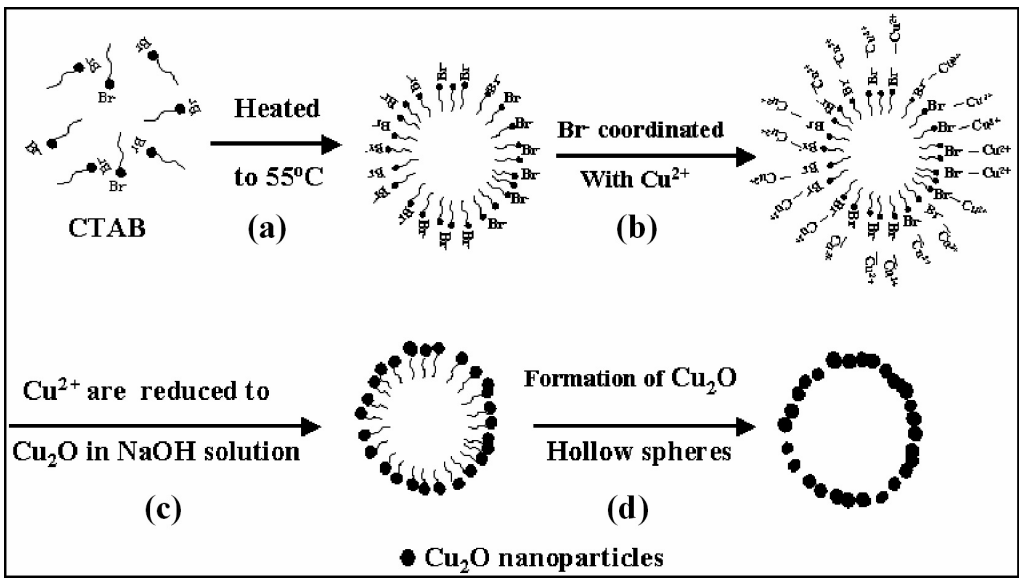

Figure 8. Schematic illustration of the formation of hollow nanoparticles.

smaller particles are produced. With the increase of CTAB concentration adequate surfactant CTAB caps the surface of the Cu_2O particles because a large amount of CTAB exists in the solution, which confines the reaction and forms uniform cubic nanoparticles that mirror the fundamental cubic crystal structure of the cuprite unit cell [8]. In comparison with the porous nanocubes prepared without CTAB, the CTAB acts as a template as well as a surfactant to enhance the incorporation of the Cu_2O nuclei formed in the solution.

4. Conclusions

Various morphologic Cu_2O nanoparticles have been synthesized using a simple solution phase route. When prepared without CTAB, porous Cu_2O polycrystalline nanocubes formed with an edge length ranging from 20 to 100 nm. In low CTAB concentration, well-defined hollow Cu_2O irregular polyhedral nanoparticles formed with a preferred $\langle 111 \rangle$ orientation; with an increase of CTAB concentration to 0.03 M, nanocubic Cu_2O formed with a $\langle 001 \rangle$ orientation and highly uniform in size. The prepared Cu_2O nanoparticles are capped by a thin CuO shell, which was formed by the adsorbed oxygen modifying the Cu_2O surface layer and can enhance the stability of the Cu_2O nanoparticles. UV–visible absorption spectra indicate both the hollow and cubic Cu_2O nanostructures have blue shift effects.

Acknowledgments

We thank H C Yu, R J Xiao, H Y Chen, L B Liu, X A Yang and Y Li for their assistance in experiments and useful discussions.

References

[1] Puntes V F, Krishnan K M and Alivisatos A P 2001 *Science* **291** 2115
[2] Sun S H and Zeng H 2002 *J. Am. Chem. Soc.* **124** 8204
[3] Sun Y G and Xia Y N 2002 *Science* **298** 2176
[4] Manna L, Milliron D J, Meisel A, Scher E C and Alivisatos A P 2003 *Nat. Mater.* **2** 382
[5] Milliron D J, Hughes S M, Cui Y, Manna L, Li J B, Wang L W and Alivisatos A P 2004 *Nature* **430** 190
[6] Switzer J A, Hung C J, Huang L Y, Switzer E R, Kammler D R, Golden T D and Bohannan E W 1998 *J. Am. Chem. Soc.* **120** 3530
[7] Briskman R N 1992 *Sol. Energy Mater. Sol. Cells* **27** 361
[8] Gou L F and Murphy C J 2003 *Nano Lett.* **3** 231
[9] Bohannan E W, Shumsky M G and Switzer J A 1999 *Chem. Mater.* **11** 2289
[10] Wang W Z, Wang G H, Wang X S, Zhang Y J, Liu Y K and Zheng C L 2002 *Adv. Mater.* **14** 67
[11] Chen Z Z, Shi E W, Zheng Y Q, Li W J, Xiao B and Zhuang J Y 2003 *J. Cryst. Growth* **249** 294
[12] Wu Z C, Shao M W, Zhang W and Ni Y B 2004 *J. Cryst. Growth* **260** 490
[13] Caruso F, Caruso R A and Möhwald H 1998 *Science* **282** 1111
[14] Yin Y D, Rioux R M, Erdonmez C K, Hughes S, Somorjai G A and Alivisatos A P 2004 *Science* **304** 711
[15] Mclntyre N S, Sunder S, Shoesmith D W and Stanchell F W 1981 *J. Vac. Sci. Technol.* **18** 714
[16] Ghijsen J, Tjeng L H, van Elp J, Eskes H and Czyzyk M T 1988 *Phys. Rev.* B **38** 11322
[17] Balamurugan B, Metha B R and Shivaprasad S M 2001 *Appl. Phys. Lett.* **79** 3176
[18] Braun P V and Stupp S I 1999 *Mater. Res. Bull.* **34** 463
[19] Zheng X Z, Xie Y L, Zhu Y, Jiang X C and Yan A H 2002 *Ultrason. Sonochem.* **9** 311